

Detection and Improvement of Power Quality Disturbances using Wavelet Transform with Noise-Suppression Method

N.V.H.Ravikumar¹, Dr.CH.Sai Babu², K. Durga Syam Prasad³

¹PG Student, Department of EEE, JNTUK College of Engineering, Kakinada-533003, INDIA

²Professor, Department of EEE, JNTUK College of Engineering, Kakinada-533003, INDIA

³Ph.D. scholar, Department of EEE, JNTUK College of Engineering, Kakinada-533 003, INDIA

Abstract—Recently power quality has become one of the most important issues in modern power industry. The origin of events which affect quality of power is mainly electromagnetic transients, harmonic distortion in addition to voltage sag, swell, flicker, and other power quality disturbances that proliferate in modern electric power grids. The WT is offering a large variety of potential bases, where optimization can be further performed. In the WT applications the process often confuses the transient signals and the noises ride on the signals. Consequently, the threshold is difficult to give in detecting the existence of transient signals. To eliminate the difficulty of distinguishing the signals from the noises existing in the Wavelet Transform Coefficients (WTCs) of the signals, a denoising algorithm is presented to suppress the noise riding on the signals. To further improve the disturbance detection rate by more effectively discriminating the signals from the noises after the DWT, a spatial-correlation-based noise-suppression algorithm is proposed in this paper.

This work describes the techniques of correcting the supply voltage sag, swell in a distributed system. At present, a wide range of very flexible controllers, which capitalize on newly available power electronics components, are emerging for custom power applications. Among these, the distribution static compensator is the most effective devices. A D-STATCOM injects a current into the system to correct the voltage sag, swell. Comprehensive results are presented to assess the performance of device as a potential custom power solution.

Keywords—Noise measurement, power quality, wavelet transform, D-STATCOM, Voltage dips, swells, interruption, and power system monitoring.

I. INTRODUCTION

In the deregulated power market, the quality of power has a direct economic impact on utilities and industrial customers. With the increase in the use of more modern equipment and more automation, there is a growing concern about power quality (PQ) and its automatic monitoring and analysis has become an important challenging issue for power engineers. To upgrade the PQ, monitoring the power signals in a wide range and a long run is evitable to find out the real causes of the PQ problem. While monitoring fault recorder should capture only the waveform cycles covering the disturbance in order to reduce the volume of data to be recorded and analyzed. Therefore, only the portion of the

signals covering the disturbances should be detected and saved for further investigation of the PQ problems.

In general, there are three steps to address the PQ problems, which are detection, localization, and classification. The frequency and time domain information is needed to complete the three steps. To analyze the PQ, feature extraction is the key point. The extraction of the features of the disturbances requires its time domain duration estimation, suitable transformation, and observation of the signals after transformation. Various transformation methods have been proposed for detecting and localizing the PQ events, which include the Discrete Fourier Transforms (DFT), Short-Time Fourier Transform (STFT) and the Wavelet Transform (WT).

Traditionally, by extracting the frequency contents of the recorded signals, the DFT has been used for the steady-state analysis of the power harmonics. According to the frequency contents of the signals, some of the PQ problems related to harmonics can be detected. Nevertheless, with its constant bandwidth, the DFT is not suitable for the detection of the short term transient signals. Moreover, the time-evolving effects of the frequency in nonstationary signals are not considered in the DFT techniques.

If the amplitude of a harmonic signal fluctuates with time, the FT cannot be used without modification. A method commonly used is to window the signal into a sequence of sufficiently small that the waveform approximates a stationary waveform. This approach is known as a short-time FT (STFT). This approach has the effect of giving some time resolution to the measurement at the expense of frequency resolution. The limitation of a fixed window width, in fact, is inadequate for the analysis of the transient nonstationary signals. The STFT will work well provided the window is short enough compared with the fluctuation rate. High rates of fluctuation can give rise to significant errors.

Wavelet transforms (WTs) have emerged as fast and effective tools for automated detection and more efficient characterization of the PQ disturbances, in power system protection. Discrete wavelet transform (DWT)based multi resolution analysis (MRA), which is also referred to as multi resolution signal decomposition (MSD) in PQ literature, analyzes the signal at different frequencies with different resolutions. Since the WT is offering a large variety of potential bases, where optimization can be further performed. Multi resolutions of both time and frequency are prepared in the WT approach. A greater resolution in time is provided for

the high-frequency components of a signal, and a greater resolution in frequency is provided for the low-frequency components. With the multi resolution characteristics, the WT is considered very adequate for the analysis of the power system transients due to various disturbances.

The presence of noise not only degrades the detection capability of wavelet and other higher time resolution-based PQ monitoring systems but also hinders the recovery of important information from the captured waveform for time localization and classification of the disturbances. In actual applications, the process often confuses the transient signals and the noises riding on the signals. Consequently, the threshold is difficult to give in detecting the existence of transient signals.

To further improve the disturbance detection rate by more effectively discriminating the signals from the noises after the DWT, a spatial-correlation-based noise-suppression algorithm is proposed in this paper. By making use of the spatially selective noise-filtration technique, the proposed algorithm calculates the corresponding correlation coefficients from the WTCs of the signals at several adjacent scales. The time points with higher correlated WTCs at the adjacent scales indicate the fact that a significant signal variation or a transient event exists. Accordingly, the approach can avoid the effects of the noises on the detection of the transient signals.

Utilities often focus on disturbances from end-user equipment as the main power quality problems. This is correct for many disturbances, flicker, harmonics, etc., but voltage dips mainly have their origin in the higher voltage levels. If the economical losses due to voltage dips are significant, mitigation actions can be profitable for the customer. There are different ways to mitigate voltage dips, swell in transmission and distribution systems. At present, a wide range of very flexible controllers, which capitalize on newly available power electronics components, are emerging for custom power applications. Among these, the distribution static compensator is most effective devices, which is based on the VSC principle. A new PWM-based control scheme has been implemented to control the electronic valves in the two-level VSC used in the D-STATCOM.

II. WAVELET EXPLANATION

Due to its ability to extract time and frequency information of signal simultaneously, the WT is an attractive technique for analyzing PQ waveform. WT can be continuous or discrete. Discrete WT (DWT) can be viewed as a subset of Continuous WT (CWT). Based on the characteristics of the band pass filters, the WT has been proposed to investigate the transient phenomena of the power signals from different scales of the WTCs. In practical applications, the DWT is commonly used. The DWT uses the low-pass $h(k)$ and the high-pass $g(k)$ filters to divide the frequency-band of the input signal $f(k)$ in respective low- and high-frequency components into octave bands. The low-pass filter $h(k)$ is determined from the scaling function. The high-pass filter $g(k)$ is determined

from both the wavelet and scaling functions. The wavelet and scaling functions are, respectively, given as,

$$\begin{aligned} \psi(k) &= \sqrt{2} \sum_n g(n) \phi(2k - n), \\ \phi(k) &= \sqrt{2} \sum_n h(n) \phi(2k - n), \end{aligned} \quad (1)$$

where n is integers and represent the number of samples. While the low-pass filtering produces the approximations A_j , the high-pass filtering produces the details D_j of the decomposition. The relationship of the approximation coefficients and detail coefficients between two adjacent levels are given as,

$$\begin{aligned} A_{j+1}(k) &= \sum_n h(n - 2k) A_j(n), \\ D_{j+1}(k) &= \sum_n g(n - 2k) A_j(n), \end{aligned} \quad (2)$$

where j is frequency band level.

In particular, the transient problems with high-frequency components can be detected and located through an adequate scale of WTCs. The WMRA is based on decomposition of the original signal into different signals at various levels of resolution. In essence, it is represented by one set of scaling coefficients, and one or several sets of wavelet coefficients,

$$f(k) = \sum_n A_1(n) \phi(k - n) + \sum_n \sum_{j=1} D_j(n) 2^{-j/2} \psi(2^j k - n). \quad (3)$$

There are many wavelet functions named as mother wavelets. The choice of mother wavelet is important because different types of mother wavelets have different properties. Several popular wavelet functions are Haar, Morlet, Coiflet, Symlet and Daubechies wavelets.

A dyadic DWT of discrete time sequence $f(k)$ of length N is essentially a decomposition of the spectrum of $f(k)$; $F(w)$ into orthogonal subbands defined by

$$\frac{1}{2^{m+1}T} \leq w \leq \frac{1}{2^m T}, m = 1, 2, \dots, J$$

Where T is the sampling period associated with $f(k)$ and represents the total number of resolution levels.

Let $\psi(t)$ be a mother wavelet, and its FT can be shown as

$$\hat{\psi}(w) = \langle \psi(t), e^{jw t} \rangle = \int_{-\infty}^{\infty} \psi(t) e^{-jw t} dt. \quad (4)$$

After the operation of dilation and translation, (4) can be written as a baby wavelet shown in the following:

$$\psi_{ab}(t) = \frac{1}{\sqrt{a}} \psi\left(\frac{t-b}{a}\right), a \in R^+, b \in R \quad (5)$$

Where a is a scaling factor and b is a translating factor. The FT of (5) can be described in

$$\hat{\psi}_{ab}(w) = \frac{1}{\sqrt{a}} \int_{-\infty}^{\infty} \psi\left(\frac{t-b}{a}\right) e^{-jw t} dt$$

$$= a \left|a\right|^{-\frac{1}{2}} \hat{\psi}(aw) e^{-jwb} \quad (6)$$

The continuous WT (CWT) of a time-continuous signal x_t is defined as

$$F_{x_{t_{cwt}}}(a, b) = |a|^{-1/2} \int_{-\infty}^{\infty} x_t \psi^* \left(\frac{t-b}{a} \right) dt \quad (7)$$

where $F_{x_{t_{cwt}}}(a, b)$ is the CWT of signal x_t with wavelet $\psi(t)$ and parameters a and b . The asterisk in (7) denotes a complex conjugate operation. In this paper, the Daubechies's wavelets with a four-coefficient filter (D4 wavelet) are used as a mother wavelet. For a mother wavelet $\psi(t)$ given in (7), different scaling and translating factors can lead to scales of frequency bands at levels of resolutions. In practical applications, the continuous wavelet function can be transferred to a discrete form via a sampling way. In (8), the factors a and b are replaced by a_0^m and $na_0^m b_0$, respectively, where $m, n \in Z$ and Z is a set of integers. Then, (8) can be written into a general discrete form

$$\psi_{mn}(t) = a_0^{-m/2} \psi(a_0^{-m} t - nb_0), a_0 > 1, b_0 \neq 0. \quad (8)$$

The DWT of the sampled signals x_n is employed to replace the CWT operation of x_t in (4)

$$DWT_x(m, n) = \frac{1}{\sqrt{2^m}} \sum_k x_k \psi^* \left(\frac{k-n}{2^m} \right) \quad (9)$$

where k is an operating index; m is a scaling number; n is a sampling time point, $n = 1, 2, \dots, N$; and N is the number of sampling points. The factors a and b in (7) are expressed using integer parameters m and n through $a = 2^m$ and $b = n$ (thereby, a dyadic transformation), respectively, in the DWT. Based on (9), the DWT of x_n , $n = 1, 2, \dots, N$, proceeds successively with various band pass filtering effects. At the first stage, the time-stamped data ($m = 1$ for scale 1) out of the filtering operation extract the highest frequency components from the signal. Moreover, the output data for the scale 2 WTCs denote the second higher frequency band. The procedure continues until the highest scale ($m = M$) is reached.

As described earlier, because diverse frequency components, especially higher frequency, often exist in the signals of disturbance events, thus examining scales of the WTCs would help determine the occurrence of the disturbance events as well as their occurring time. In determining the occurrence of a disturbance event, thresholding the WTCs is one of the most common approaches adopted in the literature. The WTCs that are larger

than the given threshold values indicate the start or end points of the disturbance events. Counting on this, the DWT techniques have been widely used to analyze the disturbance events in the power systems.

III. NOISE EXPLANATION

A. SNR Ratio

To test the effectiveness of the proposed technique, simulated PQ disturbances have been considered. The simulated PQ disturbances include pure sine wave, voltage sag, voltage swell, oscillatory transients and sustained interruptions. All simulated waveforms are obtained for a power frequency, and are normalized with a normal sinusoidal voltage without any disturbance before they are processed through the proposed denoising module for testing. Another important issue related to the proposed method is noise which is generally omnipresent in an electrical power distribution network. Therefore, the performance of proposed algorithm was tested in different noise environments. Gaussian white noise is widely used in the researches on the PQ issues. The value of SNR is defined as follows:

$$SNR = 10 \log (P_S/P_N) \text{ dB}$$

where P_s is the power (variance) of the signal and P_n is that of the noise. The noise was added with three phase signals of the events. Event signals were tested by adding 35, 40, 45 and 50 Db of noise.

B. Noise Suppression Algorithm

Although the DWT exhibits its great power in the detection and localization of the disturbance, its ability is often degraded due to the noises riding on the signal. To overcome the difficulties of capturing the disturbances out of the background noises in a low-SNR environment, a noise-suppression algorithm is proposed to be integrated with the DWT described earlier. The steps of the noise-suppression algorithm adapted from are described as follows.

Step 1: Calculate the correlations $WTR_k(m, n)$ of adjacent Scales

$$WTR_k(m, n) = DWTx(m, n) \cdot DWTx(m+1, n) \cdot \dots \cdot DWTx(m+k-1, n)$$

$$= \prod_{i=0}^{k-1} DWTx(m+i, n) \quad (10)$$

s.t. $m < M - k + 1$

where k is the number of scale inter multiplication and M is the number of all scales. The effectiveness of the step is to augment the disturbance phenomena in the scales of the WT. The correlation function $WTR_2 = DWTx(1, n) \cdot DWTx(2, n)$, ($k = 2$), is enhanced at the points corresponding to the main WTC pulses of the disturbances, but simultaneously, it is

suppressed at the points corresponding to the background noises of the signals. Nevertheless, the background noises still exist in the current WTR_2 functions obtained in the step. In the next step, a scheme is proposed to further strengthen the correlated features of the disturbances to distinguish the significant disturbance signals from the noises.

Step 2: Calculate the new values of $WTR_{new,k}(m, n)$

$$WTR_{new,k}(m, n) = WTR_k(m, n) * \sqrt{\frac{P_{DWT}(m)}{P_{WTR}(m)}}$$

where $P_{WTR}(m) = \sum_n WTR_k^2(m, n)$ and

$$P_{DWT}(m) = \sum_n DWT_x^2(m, n). \tag{11}$$

$WTR_{new,k}$ is adaptively strengthened at the sharp pulses of the m^{th} scale WTCs through the WTR_k and the factor of

$$\sqrt{\frac{P_{DWT}(m)}{P_{WTR}(m)}}.$$

Step 3: Extract the disturbances from the noise-riding signals at scale m through the following procedure:

MASK(m, n) = 0;

For m = 1 : M

For n = 1 : N

If $|WTR_{new,k}(m, n)| > |DWT_x(m, n)|$

Then { $WTR_{new,k}(m, n) = 0;$

$DWT_x(m, n) = 0;$

$MASK(m, n) = 1; }$

End

End. (12)

As described earlier, the main pulses are extracted by comparing the absolute values of $WTR_2(1, n)$ and $DWT_x(1, n)$ by setting $k = 2$ and $m = 1$. The pulses are now masked with the symbol $MASK(1, n) = 1$. At fine scales, except for disturbances, WTCs only have noises. By comparing the values of $|WTR_{new,k}(m, n)|$ and $|DWT_x(m, n)|$ directly, many noises may be extracted as significant disturbances. To avoid this situation, $|DWT_x(m, n)|$ can multiply by a weight of $\lambda(m)$, $\lambda(m) \geq 1$. Through this scheme, only when $|WTR_{new,k}(m, n)| \geq \lambda(m)|DWT_x(m, n)|$ is to come into existence, $DWT_x(m, n)$ is just regarded as the main PQ disturbance features. In a simulated test, setting the weights $\lambda(m)$ equal to [1.15, 1.06, 1, 1, . . . , 1], the accuracy of the PQ monitoring results are reasonable. The results will be discussed in the next section.

Step 4: Create a new $DWT_{x_{new}}(m, n)$ of all scales

If $P_{DWT}(m) < THR(m)$

Then $DWT_{x_{new}}(m, n) = MASK(m, n) * DWT_x(m, n)$

Else $DWT_x(m, n) = DWT_{x_{new}}(m, n)$, go to Step 1

(13)

Where $THR(m)$ is a preset threshold value for scale m .

For instance $MASK(1, n)$ and $DWT_{x_{new}}(1, n)$ after the first run are obtained to extract the significant disturbance signals by referring to $WTR_2(1, n)$ and $DWT_x(1, n)$. This procedure of signal compression and disturbance information extraction is iterated until the sum of the power of the unextracted points at $DWT_x(1, n)$ is less than some reference noise power at the first scale.

Step 5: Stopping condition. Repeat the procedure until all of the scales have been calculated. The flowchart of the proposed noise-suppression algorithm is shown in Fig. 1. However, in the procedure described earlier, the average power $THR(m)$ of the noises at each scale is not given in Step 4. The average power of the noises can be used as a threshold by estimation as stated in the next section.

Estimating the Average Power of the Noises:

It is well known that the standard deviation σ of a sequence $X \sim N(0, \sigma^2)$ can be estimated as $\sqrt{P_{DWT} / N}$, where $P_{DWT} = \sum_n x(n)^2$ and N is the sampling points. Assume that K points had been extracted from the sequence X , and then, the discrete wavelet coefficients $DWT(m, n)$ can be written as $DWT'(m, n)$. In the meantime, $DWT'(m, n)$ can be regarded as all produced from noises. Currently, the variance σ_m^2 can be estimated as $P'_{DWT}(m)/(N - K)$, and hence, the average power of the noises is $(N - K) \sigma_m^2$.

In fact, $DWT'(m, n) = DWT'_s(m, n) + DWT'_n(m, n)$, where $DWT'_s(m, n)$ and $DWT'_n(m, n)$ represent the WTCs of the power signals and noises, respectively. Therefore, $P'_{DWT}(m)$ can be written as follows:

$$\begin{aligned} P'_{DWT}(m) &= (N - K) \cdot E \{ DWT'(m, n)^2 \} \\ &= (N - K) \cdot E \{ DWT'_s(m, n)^2 + DWT'_n(m, n)^2 \\ &\quad + 2DWT'_s(m, n)DWT'_n(m, n) \} \\ &= (N - K) \cdot E \{ DWT'_s(m, n)^2 \} + (N - K) \cdot \sigma_m^2. \end{aligned} \tag{14}$$

$E \{ DWT'_s(m, n)^2 \}$ is always positive. However, $(N - K) \sigma_m^2$ cannot all be treated as noises in the coarse scales. To overcome this problem, $(N - K) \sigma_m^2$ can multiply a factor $th(m)$, $th(m) > 1$. Nevertheless, $E \{ DWT'_s(m, n)^2 \}$ changes with various power signals, so $th(m)$ is a variation. Luckily, setting the threshold value is not sensitive to extracting the features from the WTCs when the power system occurs in the PQ events.

It is not hard to realize that, as $E \{ DWT'_s(m, n)^2 \}$ increases, then, σ_m^2 decreases with scale. Hence, σ_m^2 is donating $P'_{DWT}(m)$ in fine scale and vice versa. The $th(m)$ can be given as follows:

$$th(1) = 1.1 - 1.2 \quad th(2) = 1.2 - 1.4 \quad th(3) = 1.4 - 1.6$$

When $m > 3$, $th(m) = 1.6 - 1.8$.

The threshold $THR(m)$ in Step 4 can be adjusted to be $THR(m) = (N - K) \sigma_m^2 * th(m)$. Due to noise donating at fine

scales, σ_m^2 can be estimated from the first two scales of the DWT coefficients. If $|WTR_{new,2}(1, n)| > \lambda(1)/DWT_2(1, n)$, then set the corresponding n points in $DWT_2(1, n)$ to be zero. Therefore, assume that k points have been removed from the sampling points, and $\tilde{DWT}_2(1, n)$ can be regarded as that produced by noises.

Hence, the power of $\tilde{DWT}_2(1, n)$ can be written as $\tilde{P}_{DWT}(1)$, and the variance is $\sigma_1^2 = \tilde{P}_{DWT}(1)/(N - K)$. In a similar way, the variances of all DWT scales can be shown to be the same with scale 1, i.e., $\sigma_1^2 = \sigma_2^2 = \dots = \sigma_M^2$.

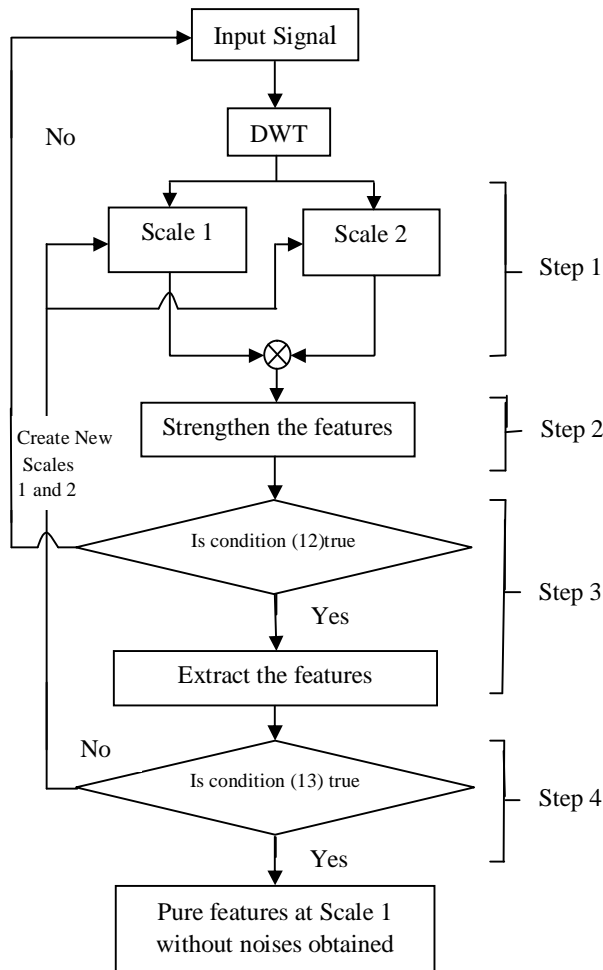


Fig. 1. Flowchart of the proposed noise-suppression algorithm.

IV. PROPOSED SYSTEM.

A. Explanation of Layout

The proposed system is as shown in fig.2. The circuit contains power generating station, transmission line, circuit breakers (for sag and swell) and generator with cyclo convertor.

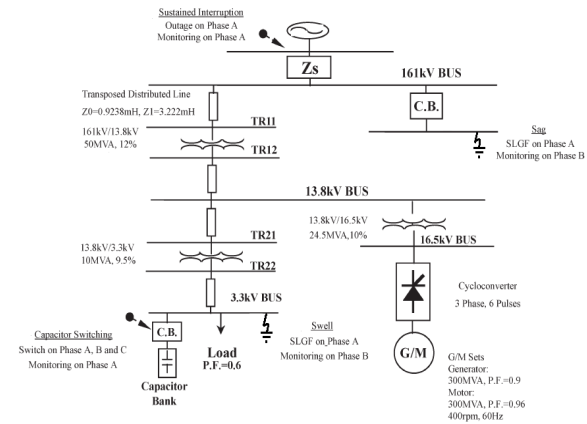


Fig.2. Diagram of the circuit for the simulations

The disturbances which are to be analysed are presented in system caused by faults, sudden change in steady state condition and malfunction of protective device. Simulated voltage-sag signal caused by the single-line ground fault (SLGF) that occurred on phase A and monitored on phase B for 0.1 s, and then, the system recovered to be normal again. The signal simulating the voltage-swell disturbance on a 3.3-kV bus and the signal with the peak value is larger than the normal, which is caused by the SLGF on phase A and monitored on phase B as shown in circuit.

A transient disturbance is a sudden non power frequency change in the steady-state condition of the voltage, current or both. Lighting or capacitor energization usually causes the impulsive or oscillatory transients, whose duration lasts for a few microseconds to milliseconds. The impulses riding on the power-frequency signal due to capacitor switching are simulated at the capacitor bank as shown in circuit. A sustained interruption is defined as that when the supply voltage decreases to less than 10% of the normal for a duration exceeding 1 min. The interruption disturbance is usually caused by a fault in the power systems, failure of the equipment, or malfunction of the protective device. Simulated sustained interruption signal, with the voltage dropping to zero due to a fault in the generator.

As explained in previous sections DWT is applied to these disturbance signals. Scales 1 and 2 of the WTCs are occurred. In order to improve the performance of WT technique in processing the noise riding signals, Spatial noise-suppression algorithm integrates with DWT as explained in section III.B (Noise Suppression Algorithm).Using (10)–(11)

of the noise-suppression scheme, the WTR_2 occurred. However, it still remains difficult, as done by the computer, when the WTC magnitudes of the disturbance and the noises are variable. Through the noise-suppression scheme proposed in this paper, the WTCs are reduced. The result of the noise suppression scheme is cleaning up the noises.

However, it still remains difficult, as done by setting a suitable threshold to remove noises in different voltage levels, when the WTC magnitudes of the disturbance and the noises are variable. As we know, it is not a good idea to set a fix threshold in different voltage levels, but according to different levels, to put various thresholds is impracticable in real power systems. The noise-suppression scheme proposed in this paper has the ability to adjust an appropriate threshold automatically according to different voltage levels.

B. Simulink model

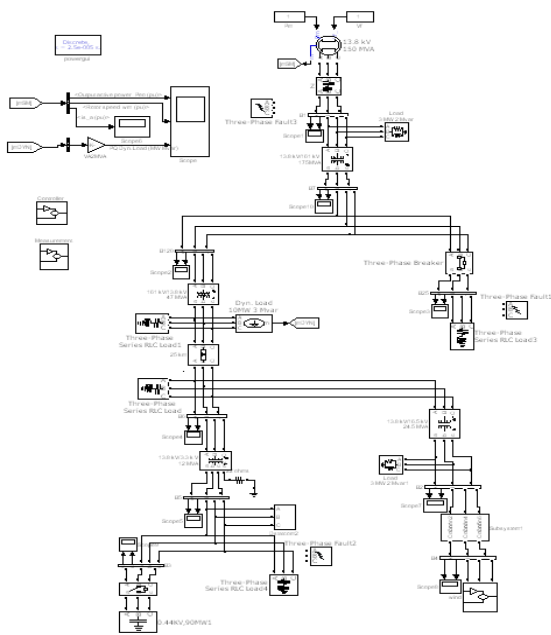


Fig.3. Simulink model for proposed circuit diagram

The simulink model for proposed circuit is as shown in fig.3. The disturbance signals from circuit are saved for analysis. These signals contain noise of 45db which is added for analysis. Application of DWT and noise-suppression algorithm is as explained earlier. Scale 1, scale2, Correlation of scales and detection of disturbances are given below.

C. Wave forms

Shown in Fig.4 the event with sag of the voltage waveform at about 0.1 s is related to sampling points. The recorded signal was then transformed into scales 1 and 2

through the DWT. Through (10)–(13), the results are shown as correlation in fig.4. Using the noise-suppression algorithm, the WTCs at the first scale after trimming the noises off are shown as disturbance in signal which pinpoints out clearly the occurring time of the voltage sag by a single impulse of the WTCs.

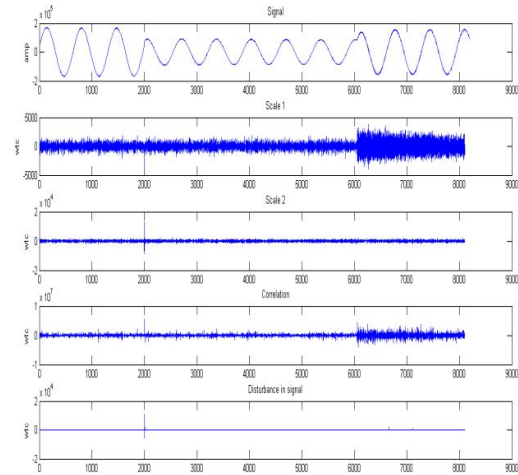


Fig.4. Noise-suppression process for the simulated sag in relation to sampling points.

Detection of swell using suppression algorithm is as shown in fig.5. Voltage waveform is related to sampling points corresponds to time. The WTCs pinpoint out the occurrence of swell at particular sampling points.

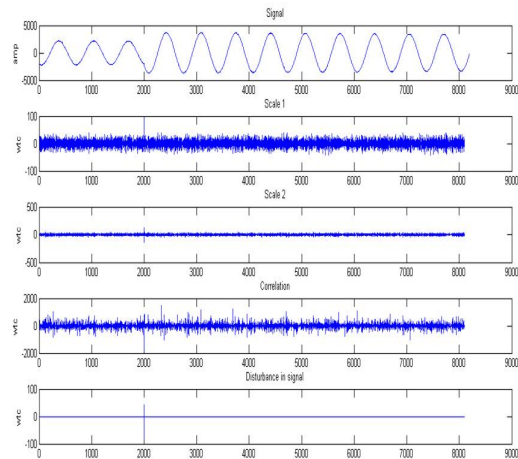


Fig.5. Noise-suppression process for the simulated swell in relation to sampling points.

The result of the noise suppression scheme in cleaning up the noises is shown in fig.6, fig.7 for oscillatory transients and sustained interruption respectively. The WTCs again provide a concise for the occurrence of the impulses.

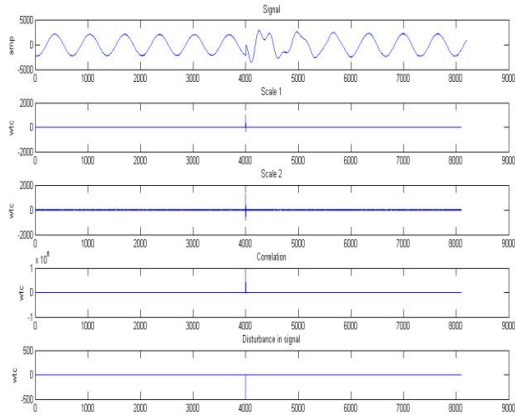


Fig.6. Noise-suppression process for the simulated oscillatory transient in relation to sampling points.

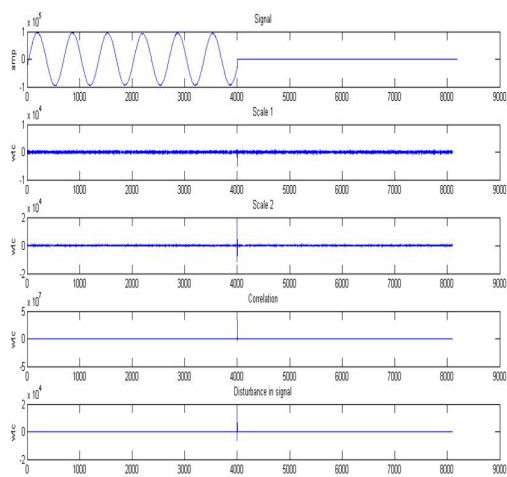


Fig.7. Noise-suppression process for the simulated sustained interruption in relation to sampling points.

Table 1 shows the WTCs of scale1 after processing through suppression algorithm. For each individual disturbance respective sampling points (corresponding to time), detailed coefficient of scale 1 after DWT, correlation values of scale 1 and scale 2, denoised coefficients (which are indicates the occurrence of disturbance in scale 1) are tabulated at noise level of 45 dB. As per the (12) in step 3 correlation values become zero when condition obeys and scale 1 coefficient values are masked with symbol MASK(1,n)=1. The remaining coefficients are treated as noise

in the signal and those are nullified. The iterative process had been taken for accurate identification of disturbances.

In table 1 coefficients of disturbance occurred are detected at 4000th sampling point for sag and swell, which are shown at 2000th sampling point in figures 5 and 6 respectively.

That means that for applying denoising algorithm the data of signal is taken between 2000-10000 sampling points which covers the disturbance. Same for Oscillatory transient and Sustained interruption also.

Disturbance	Sampling points	Detailed coefficients of scale 1	Correlation	Denoised coefficients
Sag	2000	-792.55002	-1075.5774	0
	3000	-286.377537	14209.2428	0
	3999	-6583.9436	0	-5806.82230
	4000	12844.27794	0	12678.95048
	6000	105.7211754	50733.6139	0
	8000	150.789336	-151232.818	0
Swell	10000	-42.1436001	236491.3774	0
	2000	-16.7719396	-13.2813802	0
	3000	1.24540639	27.88747842	0
	3999	36.85370276	0	40.77888652
	4000	-80.2463140	0	-84.3350288
	6000	1.62886086	-6.09293851	0
Oscillatory Transient	8000	-7.06424946	3.754759185	0
	10000	-3.17737272	-110.508287	0
	2000	-34.0850897	-26713.0582	0
	3000	-15.0159288	-7.63128138	0
	4000	-15.9591444	23.32750893	0
	5999	-472.971750	0	-496.825516
Sustained Interrupt	6000	1009.602559	181744.1118	0
	8000	7.395846894	23.85089418	0
	10000	-8.93368705	-19.2599152	0
	2000	-276.255806	-276.255806	0
	3000	-139.169444	15968.87264	0
	4000	87.1354346	-12637.6387	0
Sustained Interrupt	5999	-6375.72658	0	-6375.72658
	6000	13180.74197	0	13180.74197
	8000	73.12142263	1778.254734	0
	10000	-149.954373	-52349.7704	0

Table 1. Denoised coefficients of disturbance signals at noise of 45dB.

Table 2 shows the WTCs of scale1 for each individual disturbance after processing through suppression algorithm. Denoised coefficients (which are indicates the occurrence of disturbance in scale 1) are tabulated at noise level of 50 dB, 40 dB, 35 dB.

As noted, the tolerance to noise declines as the SNR becomes smaller. The table also reveals that the tolerance to noise of the PQ monitoring system is heavily related to the types of disturbances. For the transient and interruption disturbances, the system can have a 100% detection rate for the SNR that is as low as 35 dB. Nevertheless, for that SNR value, the detection rate of the sag disturbances still has 98%

and for swell detection rate is 99%. Generally, in all of the testing cases, the PQ monitoring system with the noise-suppression scheme shows the essential capability of tolerating the potential noises contained on the signals under investigation.

Disturbance	Sampling points	Denois coefficients for 50dB	Denois coefficients for 40dB	Denois coefficients for 35dB
Sag	2000	0	0	0
	3000	0	0	0
	3999	-4856.5341	-2992.16007	-7278.35343
	4000	9608.97932	9177.87545	11341.6228
	6000	0	0	0
	8000	0	0	0
Swell	10000	0	0	0
	2000	0	0	0
	3000	0	0	0
	3999	63.4031867	65.57753218	188.8896637
	4000	-110.01984	-151.187883	-114.728972
	6000	0	0	0
Oscillatory Transient	8000	0	0	0
	10000	0	0	0
	2000	0	0	0
	3000	0	0	0
	4000	0	0	0
	5999	-480.35089	-487.261159	-460.301952
6000	0	1012.38880	1004.58276	
Sustained Interrupt	8000	0	0	0
	10000	0	0	0
	2000	0	0	0
	3000	0	0	0
	4000	0	0	0
	5999	-6106.0346	-5040.50951	-5674.89315
6000	12685.1724	12317.26022	13991.10941	
8000	0	0	0	
10000	0	0	0	

Table 2. Denois coefficients of disturbance signals at noise levels of 50 dB, 40 dB, 35 dB.

D. D-STATCOM

A D-STATCOM (Distribution Static Compensator), which is schematically depicted in Figure 8, consists of a two-level Voltage Source Converter (VSC), a dc energy storage device, a coupling transformer connected in shunt to the distribution network through a coupling transformer. The VSC converts the dc voltage across the storage device into a set of three-phase ac output voltages. These voltages are in phase and coupled with the ac system through the reactance of the coupling transformer. Suitable adjustment of the phase and magnitude of the D-STATCOM output voltages allows effective control of active and reactive power exchanges between the D-STATCOM and the ac system. Such configuration allows the device to absorb or generate controllable active and reactive power.

The D-STACOM employs an inverter to convert the DC link voltage V_{dc} on the capacitor to a voltage source of adjustable magnitude and phase. Therefore the D-STATCOM can be treated as a voltage-controlled source. Capacitor sizing

is referred to the fault current in the system. The difference in current between the current before and after the fault is considered as current faults. In capacitor sizing, a suitable range of DC capacitor is needed to store the energy to mitigate the voltage sag. The DC capacitor, CDC is used to inject reactive power to the D-STATCOM when the voltage is in sag condition. The VSC connected in shunt with the ac system provides a multifunctional topology which can be used for up to three quite distinct purposes:

1. Voltage regulation and compensation of reactive power
2. Correction of power factor
3. Elimination of current harmonics.

Distribution STATCOM (DSTATCOM) exhibits high speed control of reactive power to provide voltage stabilization, flicker suppression, and other types of system control. such device is employed to provide continuous voltage regulation using an indirectly controlled converter.

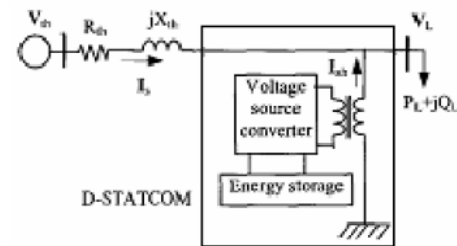


Fig.8. Schematic diagram of a D-STATCOM.

Distribution Static Compensator injected current I_{sh} corrects the voltage sag by adjusting the voltage drop across the system impedance Z_{th} . The value of I_{sh} can be controlled by adjusting the output voltage of the converter. The shunt injected current I_{sh} can be written as,

$$I_{sh} = I_L - I_s = I_L - \frac{V_{Th} - V_L}{Z_{Th}} \tag{15}$$

$$I_{sh} \angle \eta = I_L \angle -\theta - \frac{V_{th}}{Z_{th}} \angle (\delta - \beta) + \frac{V_L}{Z_{th}} \angle -\beta \tag{16}$$

The complex power injection of the D-STATCOM can be expressed as,

$$S_{sh} = V_L I_{sh}^* \tag{17}$$

It may be mentioned that the effectiveness of the D-STATCOM in correcting voltage sag depends on the value of Z_{th} or fault level of the load bus. When the shunt injected current I_{sh} is kept in quadrature with V_L , the desired voltage correction can be achieved without injecting any active power

into the system. On the other hand, when the value of I_{sh} is minimized, the same voltage correction can be achieved with minimum apparent power injection into the system. Following figure shows the simulink model of D-STATCOM which is proposed for mitigation of voltage dips.

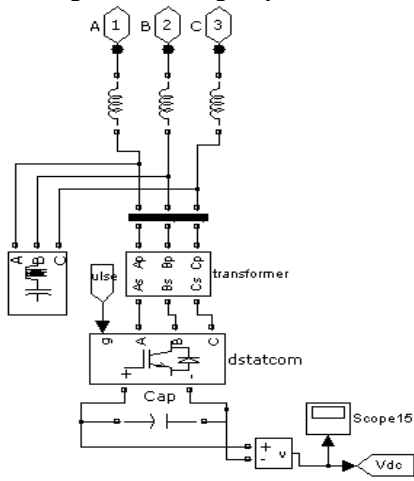


Fig.9. Simulink model of D-STATCOM.

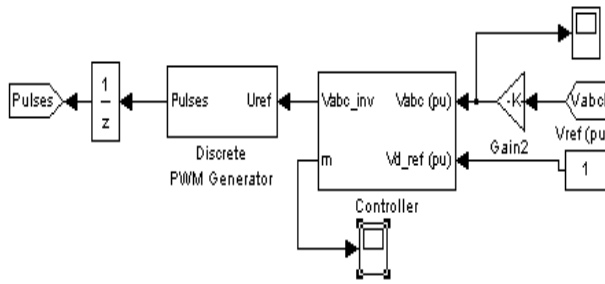


Fig.10. Simulink model of D-STATCOM controller.

The simulation of V_{rms} contains no D-STATCOM is as shown in fig.11. Sag in voltage caused by single line to ground fault during the period 0.5–0.9 s. The voltage sag at the load point is 54% with respect to the reference voltage.

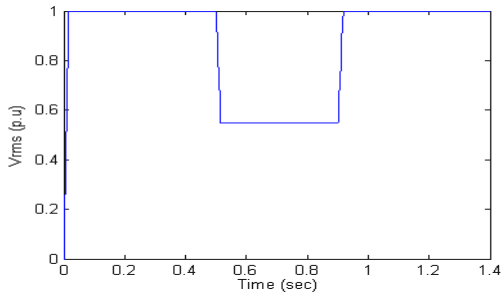


Fig.11. Voltage sag V_{rms} at the load point: Without

D-STATCOM.

A new simulations was carried out with the D-STATCOM connected to the system as shown in Figure 3 where the very effective voltage regulation provided by the D-STATCOM can be clearly appreciated.

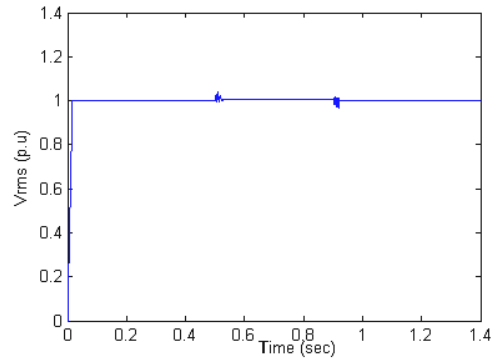


Fig.12. Voltage sag V_{rms} at the load point: With D-STATCOM.

Fig. 13 illustrates the simulation contains no D-STATCOM and single line to ground fault occurred for the period 0.5–0.9 s. The voltage swell at the load point is 58% with respect to the reference voltage. The test system for the simulation of D-STATCOM for swell is shown in Figure 14.

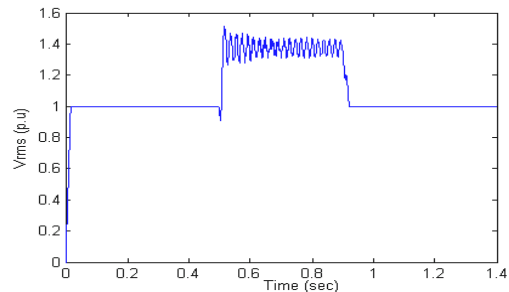


Fig.13. Voltage swell V_{rms} at the load point: Without D-STATCOM.

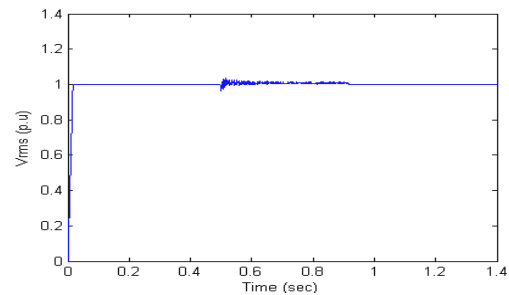


Fig.14. Voltage swell V_{rms} at the load point: With D-STATCOM.

V. CONCLUSION

To improve the abilities of the PQ monitoring spatial correlation based noise-suppression algorithm have been presented in this paper to denoise PQ waveforms. The noises mixed with the monitored signals were automatically removed according to the correlations at adjacent scales through the proposed approach. The user control in the performance of these techniques is one of the prominent advantages and provides greater flexibility compared to other denoising techniques.

The results of testing the proposed approach on the data for actual transient events showed that the PQ monitoring approach could restore the capabilities of the DWT techniques. The spatial correlation based noise-suppression algorithm, when integrated with a DWT-based PQ monitoring system, not only restores the detection and localization capability of the DWT-based monitoring system but also reduces the volume of data to be recorded. In this paper, the performance of proposed approach was tested using event signals under the conditions with noisy and noiseless. Moreover, denoising of the waveform data restores the wavelet-domain energy distribution pattern of the disturbance and will certainly increase the monitoring accuracy of the DWT-based monitoring. It has the great potential to improve the performance of the automatic PQ monitoring.

This paper has presented the power quality problems such as voltage dips, swells and interruptions, consequences, and mitigation techniques of custom power electronic device D-STATCOM. The design and applications of D-STATCOM for voltage sags, swells and comprehensive results are presented.

VI. REFFERANCES

- [1] Chiung-Chou Liao, Hong-Tzer Yang and Hsueh-Hsien Chang "Denoising Techniques With a Spatial Noise-Suppression Method for Wavelet-Based Power Quality Monitoring," *IEEE Trans.Instrum.Meas.*, Vol. 60, No. 6, July 2011.
- [2] U. D. Dwivedi and S. N. Singh, "Enhanced detection of power quality events using intra and interscale dependencies of wavelet coefficients," *IEEE Trans. Power Del.*, vol. 25, no. 1, pp. 358–366,Jan. 2010.
- [3] U. D. Dwivedi and S. N. Singh, "Denoising techniques with change point approach for wavelet-based power-quality monitoring," *IEEE Trans. Power Del.*, vol. 24, no. 3, pp. 1719–1727, Jul. 2009.
- [4] T. Tarasiuk, "Comparative study of various methods of DFT calculation in the wake of IEC standard 61000-4-7," *IEEE Trans. Instrum. Meas.*, vol. 58, no. 10, pp. 3666–3677, Oct.
- [5] W. G. Morsi and M. E. El-Hawary, "Wavelet packet transform based power quality indices for balanced and unbalanced three-phase systems under stationary or nonstationary operating conditions," *IEEE Trans. Power Del.*, vol. 24, no. 4, pp. 2300–2310, Oct. 2009.
- [6] P. S. Wright, "Short-time Fourier transforms and Wigner-Ville distributions applied to the calibration of power frequency harmonic analyzers," *IEEE Trans. Instrum. Meas.*, vol. 48, no. 2, pp. 475–478, Apr. 1999.
- [7] M. Han, Y. Liu, J. Xi, and W. Guo, "Noise smoothing for nonlinear time series using wavelet soft threshold," *IEEE Trans. Signal Process. Lett.*, vol. 14, no. 1, pp. 62–65, Jan. 2007.
- [8] Julio Barros, *Senior Member, IEEE*, and Ramón I. Diego "Analysis of Harmonics in Power Systems Using the Wavelet-Packet Transform" *IEEE Trans. instrum. meas.*, vol. 57, no. 1, Jan. 2008.
- [9] Y. Xu, J. B. Weaver, D. M. Healy, and J. Lu, "Wavelet transform domain filters: A spatially selective noise filtration technique," *IEEE Trans. Image Process.*, vol. 3, no. 6, pp. 747–758, Nov. 1994.
- [10] P. Manoj Kumar, Y. Sumanth, S. N. V. Ganesh "Improving the Power Quality by MLCI type DSTATCOM" *International Journal of Computer Applications (0975 – 8887)*, Volume 10– No.1, Nov. 2010.
- [11] E.Rambabu, E.Praveena, Prof.P.V.Kishore "Mitigation of Harmonics in Distribution System Using D – STATCOM", *International Journal of Scientific & Engineering Research* Volume 2, Issue 11, Nov.2011.